

**MECHANICAL STRUCTURE OF MERCURY'S LITHOSPHERE FROM MESSENGER OBSERVATIONS OF LOBATE SCARPS.** J. Andreas Ritzer<sup>1</sup>, Steven A. Hauck, II<sup>1</sup>, Olivier S. Barnouin<sup>2</sup>, Sean C. Solomon<sup>3</sup>, Thomas R. Watters<sup>4</sup>. <sup>1</sup>Geological Sciences, Case Western Reserve University, Cleveland, OH 44106, andreas.ritzer@case.edu, <sup>2</sup>Johns Hopkins University Applied Physics Laboratory, Laurel, MD 20723, <sup>3</sup>Department of Terrestrial Magnetism, Carnegie Institution of Washington, Washington, DC 20015 <sup>4</sup>Center for Earth and Planetary Studies, National Air and Space Museum, Smithsonian Institution, Washington, DC 20560.

**Introduction:** Laser ranging during the first two of three flybys completed by the MESSENGER spacecraft at Mercury have detected a variety of landforms interpreted to be the result of contractional tectonics, including a number of lobate scarps and wrinkle ridges [1,2]. The Mercury Laser Altimeter (MLA) has observed relief over these scarps in excess of 1 km, indicating a significant amount of contractional strain accommodation at the surface. Lobate scarps have been detected over most of the planet and are among the most visible and pervasive features observed at Mercury by the MESSENGER and Mariner 10 spacecraft [1-5] because of their significant relief, length, and broad distribution. We study thrust faulting on Mercury using finite element modeling of surface displacement fit to MLA topographic profiles, from which we constrain the extent of faulting. The maximum depth of faulting provides us with a view of the structure of Mercury's lithosphere at the time of their development [2,10].

**Laser Altimetry:** Ranging tracks from flybys 1 and 2 have provided the highest level of topographic detail to date. The MLA has thus far acquired more than 8000 measurements over the course of two equatorial flybys. The combined topographic profile from the two tracks is over 7200 km long. Several ridges and lobate scarps have been detected along each of the profiles (e.g., Fig. 1) [2].

**Finite Element Model:** The structure of the thrust faults thought to have created the lobate scarps seen on Mercury can be modeled using mechanical finite elements to constrain the geometry of the underlying fault and the behavior of the lithosphere. We used the commercially available MSC.Marc package that has been applied in several other studies [e.g., 6-9]. A thrust fault can be modeled in Cartesian coordinates at small scales as a plane in an elastic material (see Fig. 2). We approximate an elastic half-space [cf. 10] by using a large modeling domain (1200 x 300 km).

Fixed displacement boundary conditions were applied to the bottom and right edges, while a prescribed shortening was modeled as a fixed displacement at the left edge. The fault itself was modeled using gap elements as a frictionless rectangular plane. Our models assume a planar geometry, consistent with results from

previous work done by Watters et al. [10,11], modeled as plane strain 1200 km thick out of plane.

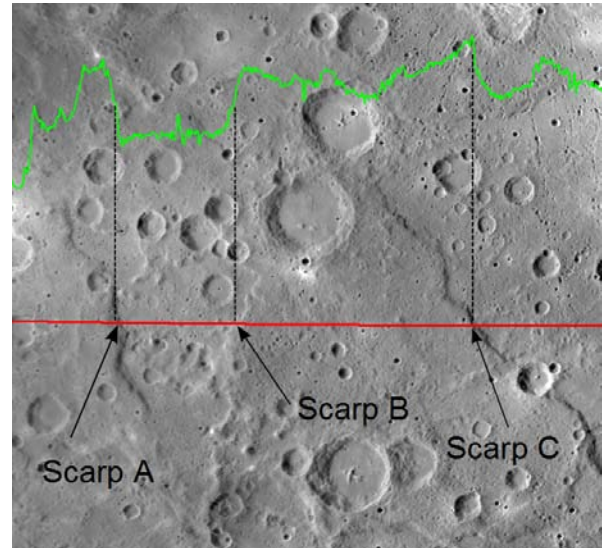


Figure 1. MDIS mosaic from the third flyby. Three lobate scarps profiled by MLA during the first flyby are labeled A, B and C. Ground track location seen in red and topographic profile is in green.

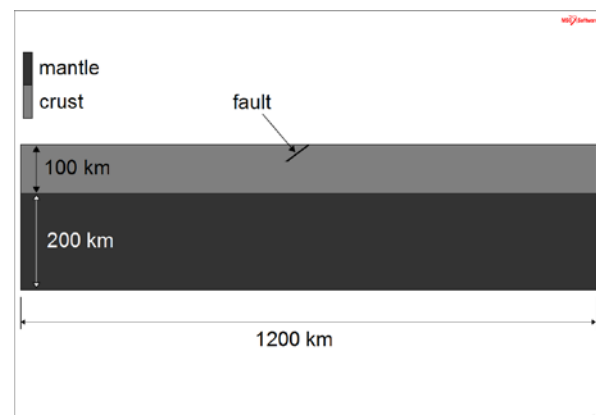


Figure 2. Finite element model of a thrust fault. To avoid overly constraining the solution, a domain 1200 km wide and 300 km deep was used. The fault can be seen at the surface as a slanted black line. Light grey is crustal material and dark grey is mantle.

We assume a surface breaking geometry, where the displacement along the fault is free, dependent only on the geometry of the fault and the amount of displacement at the left edge.

**Results:** Modeled relief is compared to the observed topography, and good fits to the faults are possible. The fault beneath scarp C (at longitude 64.7° E) is best fit by a model with a free-slip fault geometry (Fig. 3) where displacement along the fault is not restricted. The free-slip condition produces the sharp profile seen in Figure 3. The best fit geometry for this fault has a fault displacement  $d$  of 3800 m, a dip  $\theta$  of 20°, and a maximum depth of faulting  $T$  of 35 km. The fault beneath scarp B (59.3° E longitude) is also well fit by a sharp, surface-breaking fault (Fig. 3). The free-slip condition in our models differ from the model used by Watters et al. [10], who restrict the displacement over the fault by imposing a linear taper over a distance of 10 km on the fault displacement, restricting the stresses at fault tips.

The most important parameters involved in the analysis were maximum fault depth and dip angle. The effects of changing the Young's modulus or crustal thickness were negligible. Listric faulting geometries have not been investigated, but recent analysis of Beagle Rupes [12] has provided evidence for a basal decollement at that location. Models incorporating listric geometries are under investigation.

**Implications:** While the geometry of the two faults in our study differed, the best-fit models have

similar maximum depths of faulting. The depth of thrust faults on Mercury has been interpreted to be the thickness of the seismogenic lithosphere [10]. The results of this study agree with those of Watters et al. [10] despite the use of different modeling methods. Following a methodology similar to that of Watters et al. [10], lower bounds on the heat flux at the time of faulting should be around 10 mW m<sup>-2</sup> and the thermal gradient should have been at least 3 K km<sup>-1</sup>, consistent with recent dynamic strain localization models of lobate scarp development [2].

**References:** [1] Watters T.R. et al. (2009) *EPSL*, 285, 283–296. [2] Zuber M.T. et al. (2009) *Icarus*, submitted. [3] Watters T.R. et al. (2000) *GRL*, 27, 3659–3662. [4] Watters T.R. et al. (2001) *Planet. Space Sci.*, 49, 1523–1530. [5] Watters T.R. et al. (2004) *GRL*, 31, L04701. [6] Brown C.D. and Phillips R.J. (1999) *Tectonics*, 18, 1275–1291. [7] Ghent R.R. (2005) *JGR*, 110, E11006. [8] Dombard A.J. and McKinnon W.B. (2006) *J. Struct. Geol.*, 28, 2259–2269. [9] Dombard A.J. et al. (2007) *JGR*, 112, E04006. [10] Watters T.R. et al. (2002) *GRL*, 29, 10.1029/2001GL014308. [11] Watters T.R. et al. (2002) *LPS* 33, abstract #1668. [12] Rothery D.A. and Massironi M. (2009) *LPS* 40, abstract #1702.

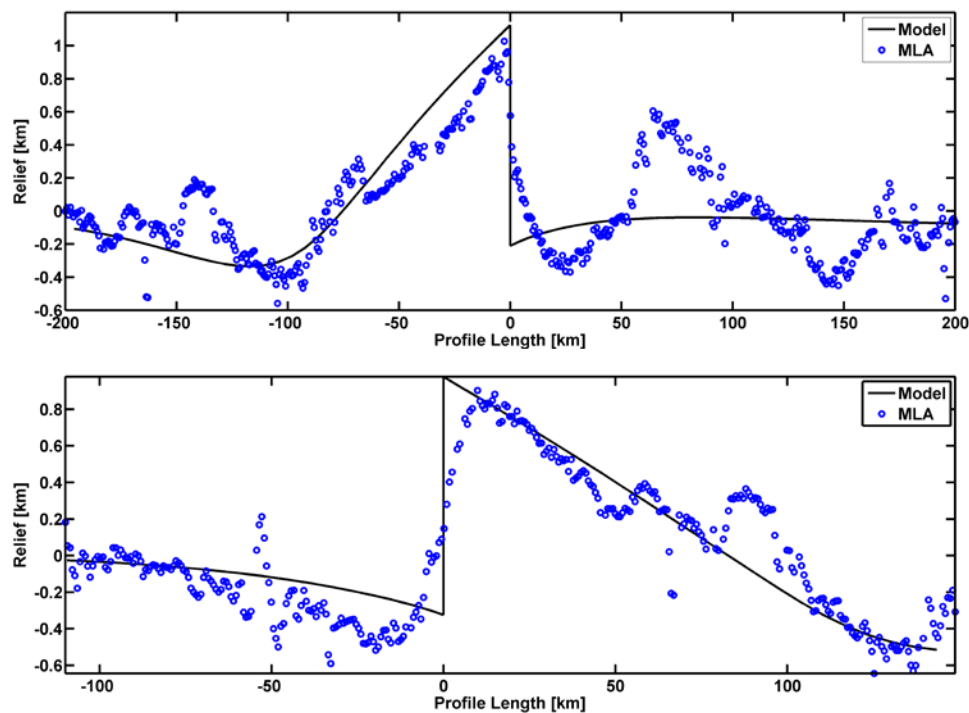


Figure 3 Upper figure shows a best-fit model (black line) for the structural relief (blue circles) at the thrust fault beneath scarp C at 64.7°E. The model shown has geometry with  $d$  of 3800 m,  $T$  of 35 km, and  $\theta$  of 20°. Lower figure shows a best-fit model (black line) for the relief (blue circles) at the thrust fault beneath scarp B at 59.3°E. This fault has geometry with  $d$  of 4200 m,  $T$  of 35 km, and  $\theta$  of 15°.